THE JOURNAL OF BIOLOGICAL CHEMISTRY
Vol. 280, No. 12, Issue of March 25, pp. 11798–11806, 2005

Printed in U.S.A.

Maize Phosphoenolpyruvate Carboxylase

MUTATIONS AT THE PUTATIVE BINDING SITE FOR GLUCOSE 6-PHOSPHATE CAUSED DESENSITIZATION AND ABOLISHED RESPONSIVENESS TO REGULATORY PHOSPHORYLATION*

Received for publication, August 2, 2004, and in revised form, January 21, 2005
Published, JBC Papers in Press, January 21, 2005, DOI 10.1074/jbc.M408768200

Akiko Takahashi-Terada‡§, Masaaki Kotera‡, Kenta Ohshima‡§, Tsuyoshi Furumoto‡, Hiroyoshi Matsumura¶, Yasushi Kai¶, and Katsura Izui‡‖

From the ‡Graduate School of Biostudies, Kyoto University, Kitashirakawa, Sakyo-ku, Kyoto 606-8502 and the ¶Graduate School of Engineering, Osaka University, Suita 565-0871, Japan

Phosphoenolpyruvate carboxylases (PEPC, EC 4.1.1.31) from higher plants are regulated by both allosteric effects and reversible phosphorylation. Previous x-ray crystallographic analysis of *Zea mays* PEPC has revealed a binding site for sulfate ion, speculated to be the site for an allosteric activator, glucose 6-phosphate (Glc-6-P) (Matsumura, H., Xie, Y., Shirakata, S., Inoue, T., Yoshinaga, T., Ueno, Y., Izui, K., and Kai, Y. (2002) *Structure* (*Lond.*) 10, 1721–1730). Because kinetic experiments have also supported this notion, each of the four basic residues (Arg-183, -184, -231, and -372′ on the adjacent subunit) located at or near the binding site was replaced by Gln, and the kinetic properties of recombinant mutant enzymes were investigated. Complete desensitization to Glc-6-P was observed for R183Q, R184Q, R183Q/R184Q (double mutant), and R372Q, as was a marked decrease in the sensitivity for R231Q. The heterotropic effect of Glc-6-P on an allosteric inhibitor, L-malate, was also abolished, but sensitivity to Gly, another allosteric activator of monocot PEPC, was essentially not affected, suggesting the distinctness of their binding sites. Considering the kinetic and structural data, Arg-183 and Arg-231 were suggested to be involved directly in the binding with phosphate group of Glc-6-P, and the residues Arg-184 and Arg-372 were thought to be involved in making up the site for Glc-6-P and/or in the transmission of an allosteric regulatory signal. Most unexpectedly, the mutant enzymes had almost lost responsiveness to regulatory phosphorylation at Ser-15. An apparent lack of kinetic competition between the phosphate groups of Glc-6-P and of phospho-Ser at 15 suggested the distinctness of their binding sites. The possible roles of these Arg residues are discussed.

Phosphoenolpyruvate carboxylase (PEPC[1]; EC 4.1.1.31) is a CO_2-fixing enzyme that yields oxaloacetate from phosphoenolpyruvate (PEP) and bicarbonate liberating P_i in the presence of Me^{2+} (1–4). PEPC is widespread not only in all photosynthetic organisms such as higher plants, algae, cyanobacteria, and photosynthetic bacteria but also in most nonphotosynthetic bacteria and protozoa. The enzyme is apparently absent in animals, fungi, and yeasts. PEPC plays primarily an anaplerotic role by replenishing C_4-dicarboxylic acids utilized for the energy and biosynthetic metabolisms.

Moreover, in higher plants, PEPC has many different physiological roles (5), which are performed by several isoforms with different catalytic and regulatory properties. The most predominant role of PEPC is its participation in the photosynthesis of C_4 plants such as maize (*Zea mays*) and sugarcane and of Crassulacean acid metabolism plants such as cactus and pineapple. In these plants, PEPC catalyzes the primary reaction to capture atmospheric CO_2 for their characteristic photosynthesis (6). In N_2-fixing legume root nodules, PEPC plays a pivotal role in carbon metabolism (7). PEPC is also involved in the maintenance of the pH balance in the cells of opening stomata, accumulation of organic acids in fruits, in the supply of organic acids exudated from roots to soil for aluminum detoxification, P_i leaching, and so on.

PEPC is usually composed of four identical subunits with a molecular mass of about 95–110 kDa. In particular, the subunit molecular size of Archaea is very small (about 60 kDa) (8, 9) and that of protozoa (malaria pathogen) deduced from its DNA sequence is very large (about 130 kDa) (www.genedb.org/genedb/malaria/index.jsp, ID: PF14_0246) . Most PEPCs studied previously have been allosteric in nature, but their effectors show a wide variety depending on the species of the organisms (1, 10), and kinetic properties modified by effectors often differ even among isoforms in the same organisms (11, 12). However, effectors of higher plant PEPCs are rather confined to a set of effectors, namely PEPC of dicot plants is activated by glucose 6-phosphate (Glc-6-P) and inhibited by L-malate or aspartate (Asp) and that of monocot plants is activated by glycine (Gly). Furthermore, higher plant PEPCs are regulated by reversible phosphorylation at Ser located near the N terminus, and this phosphorylation is catalyzed by a specific protein kinase called PEPC kinase (PEPC-k) (13–15).

Because of the enzymological and physiological importance of PEPC, and its possible usefulness in metabolic engineering (16, 17), the elucidation of its structure-function relationship has long been awaited. Recently, the three-dimensional struc-

* This work was supported in part by Grants-in-Aid for Scientific Research (B) from the Ministry of Education, Science, Sports, and Culture of Japan, a grant for the Recombinant Plant Project from the Ministry of Agriculture, Forestry and Fisheries of Japan, and a grant from Ajinomoto Co. (to K. I.). The costs of publication of this article were defrayed in part by the payment of page charges. This article must therefore be hereby marked "*advertisement*" in accordance with 18 U.S.C. Section 1734 solely to indicate this fact.

§ Supported by the 21st Century COE Program of the Ministry of Education, Culture, Sports, Science and Technology Agency of the Japanese Government.

‖ To whom correspondence should be addressed: Laboratory of Plant Physiology, Graduate School of Biostudies, Kyoto University, Kyoto 606-8502, Japan. Tel.: 81-75-753-6140; Fax: 81-75-753-6470; E-mail: izui@kais.kyoto-u.ac.jp.

[1] The abbreviations used are: PEPC, phosphoenolpyruvate carboxylase; DCDP, 3,3-dichloro-2-dihydroxyphosphinoylmethyl-2-propenoate; DTT, dithiothreitol; EcPEPC, *E. coli* PEPC; Glc-6-P, glucose 6-phosphate; PEP, phosphoenolpyruvate; PEPC-k, phosphoenolpyruvate carboxylase kinase; rEK, recombinant enterokinase; ZmPEPC, *Z. mays* PEPC isoform for C_4 photosynthesis; WT, wild type; Fru-1,6-P_2, fructose 1,6-bisphosphate.

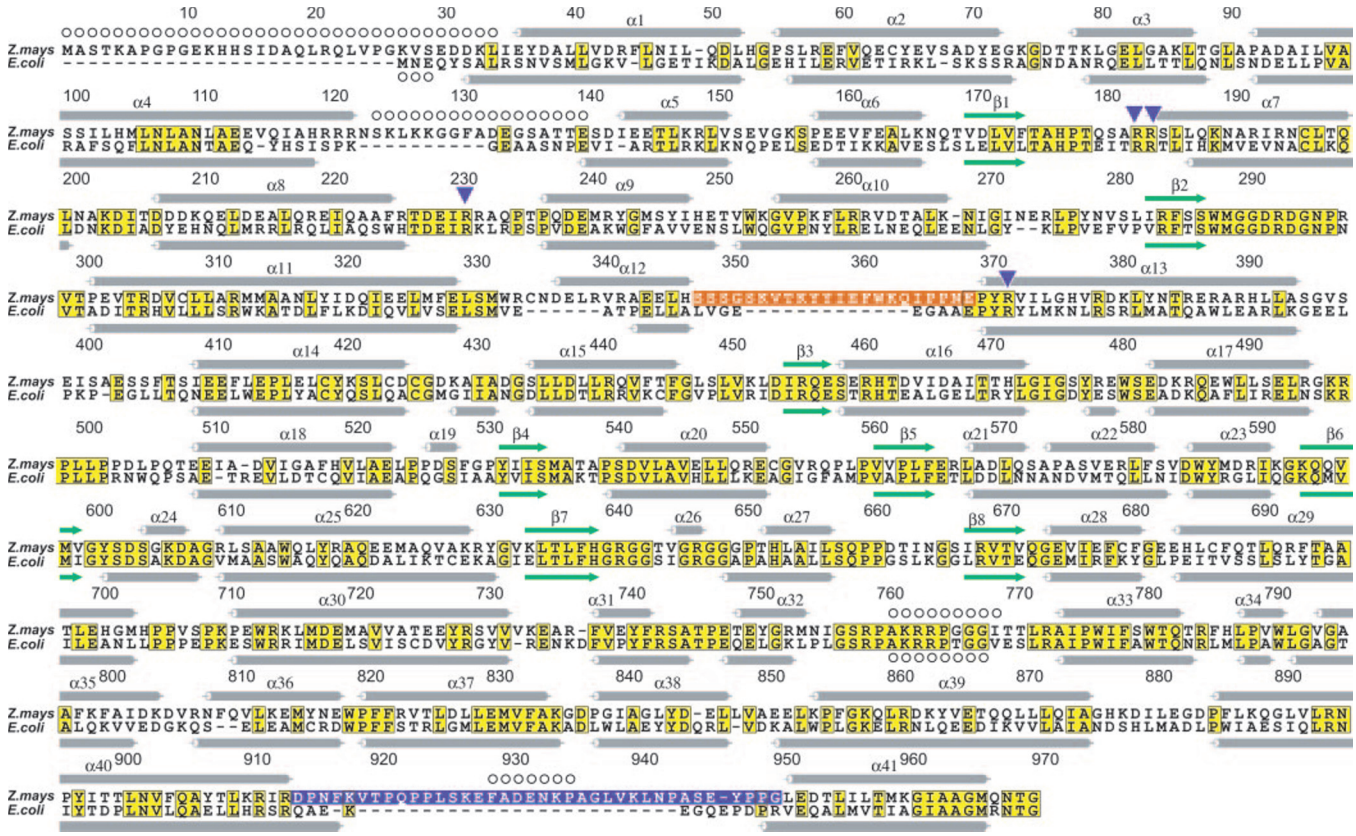

FIG. 1. **Amino acid sequence alignment and secondary structural features of ZmPEPC and EcPEPC.** The newly revised amino acid sequences of ZmPEPC (gi: 27764448 ID:ZMA536629, AC:AJ536629) and that of EcPEPC (gi: 48665 ID:ECPPCG, AC: X05903) are aligned. Secondary structural elements are indicated by *light gray cylinders* (α-helices) or *green arrows* (β-strands). The residues conserved between the two PEPCs are *boxed* in *yellow*. The residues comprising loops near the sulfate-binding site, which are specific to plant PEPCs, are shown in *reversed dark orange* or *blue violet*. The *blue violet triangles* indicate the Arg residues located at or near the binding site of sulfate anion in the crystal, which are the targets of site-directed mutagenesis in the present study. The residues for which locations could not be specified by x-ray crystallographic analysis, presumably due to their mobility in the crystal, are indicated by *open circles*. The nucleotide sequence of the cDNA (pM500) was again determined in this work, and 12 residues were corrected from the figure presented in our earlier paper (20).

ture of PEPC was solved by x-ray crystallographic analysis, as reviewed previously (4, 18). The structure of PEPC of *Escherichia coli* (EcPEPC) was thought to be in an inactive state complexed with an allosteric inhibitor, Asp (19). On the other hand, the structure of PEPC for C_4 photosynthesis from *Z. mays* (ZmPEPC) was thought to be in an activated state, because crystallization was carried out in the presence of ethylene glycol, an activating and compatible solute (20). Although identity of amino acid residues between these two enzymes is only about 40%, secondary and three-dimensional structures are very similar to each other (Fig. 1).

The catalytic site could be assigned to be above the C-terminal side of β-barrel, consistent with the data of site-directed mutagenesis (19) (Fig. 2*A*). Although the binding site for the allosteric inhibitor was disclosed in the structure of EcPEPC, the site for Glc-6-P was not known. Close examination of the structure of ZmPEPC revealed the binding of one molecule of SO_4^{2-} per subunit, which had been used as one of the precipitants for crystallization (Fig. 2, *B–D*). Because it is often the case that SO_4^{2-} binds to the site for the phosphate group of a phosphate-containing ligand in the protein crystal (21, 22), this site seemed to be a good candidate for binding with one of the allosteric activators Glc-6-P. In this work, the four Arg residues that are located at or near the binding site of SO_4^{2-} were replaced by Gln individually or in combination by site-directed mutagenesis, and the resulting mutant enzymes were investigated for their kinetic properties. Among the four ligands tested, the sensitivity to Glc-6-P was most predominantly diminished or lost, suggesting the involvement of Arg residues in the binding with Glc-6-P and/or in the transmission of allosteric signal caused by Glc-6-P. Although the mutant enzymes could be fully phosphorylated by PEPC kinase, their ability to be activated by regulatory phosphorylation was simultaneously lost. A possible mechanism for this novel finding is also discussed.

EXPERIMENTAL PROCEDURES

Enzymes and Chemicals—Oligonucleotide primers were synthesized by Proligo Primers & Probes. DNA polymerase *KOD-plus* was purchased from Toyobo. Restriction endonucleases were purchased from either Takara Bio, Inc., or New England Biolabs and were used according to the recommendations from the supplier. Recombinant enterokinase (rEK) was from Novagen. PEPC-k was kindly supplied by Y. Tsuchida of this laboratory (14). The antibodies for the phosphorylated ZmPEPC had already been prepared in this laboratory (23), and the peroxidase-conjugated AffiniPure goat anti-rabbit IgG (H + L) was from Jackson ImmunoResearch. PEP (tri-cyclohexylammonium salt) and L-malate (sodium salt) were from Sigma and Wako, respectively. 3,3-Dichloro-2-dihydroxyphosphinoylmethyl-2-propenoate (DCDP) (24) was obtained as described previously (20). All other materials were of reagent grade, and obtained as described previously (14, 25, 26) or purchased from commercial sources.

Bacterial Strains and Plasmids—*E. coli* XL1-Blue and BL21-CodonPlus (DE3)-RIL (Stratagene) were used for amplification of plasmids and expression of PEPCs, respectively. pET32a (Novagen) was used as an expression vector. pTM94 and pEM94 (27), which contain the entire coding region of the cDNA of ZmPEPC, were used as starting materials. During the course of this study, many errors were found in the sequence that had been reported by us previously (28, 29). Thus we re-determined and revised the sequence (Fig. 1). We constructed the following pTM94 and pEM94 derivatives in this work, pTMR183Q, pTMR184Q, pTMR183Q/R184Q, pTMR231Q, pTMR372Q, pEMR183Q, pEMR184Q, pEMR183Q/R184Q, pEMR231Q, and pEMR372Q.

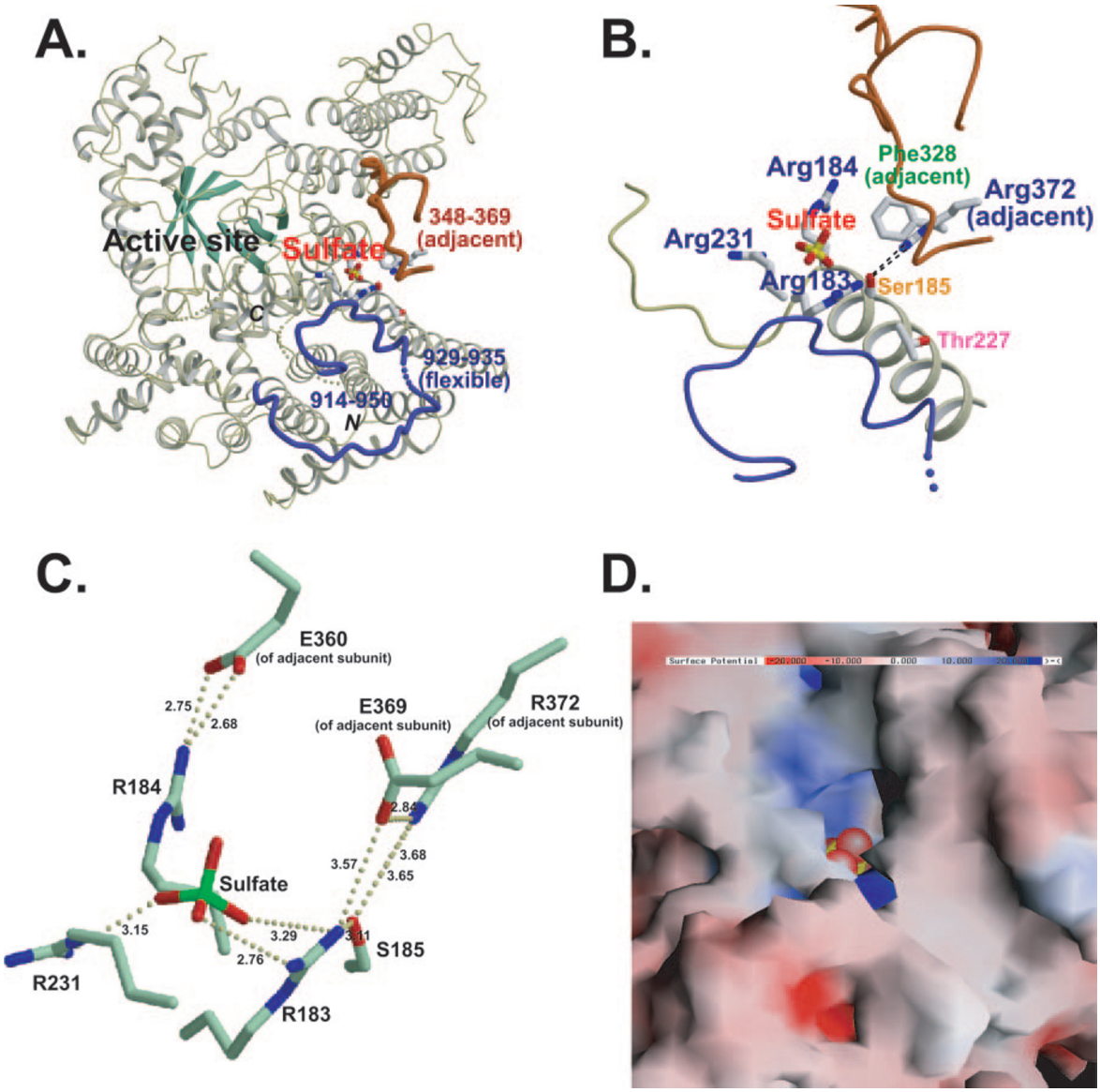

FIG. 2. **The monomeric structure of ZmPEPC and a close view of a sulfate-binding site.** *A*, ribbon model of the monomeric structure of ZmPEPC. The catalytic site is located near the C-terminal side of the β-barrel (*green arrows*). A sulfate molecule is indicated in a stick model colored in *red* and *yellow*. *Blue* and *red* structures indicate two of the three plant-specific loops (4), corresponding to the C-terminal flexible loop (residues 929–935) and the loop from the adjacent subunit, respectively. Because the N-terminal region from Met-1 to Leu-34 on which Ser-15 residues did not give reflections, presumably due to its flexibility or occasional truncation, Ile-35 is denoted as *N*. The position of the C-terminal is denoted as *C*. *B*, a close view of the sulfate-binding site. Arg residues, which are at or near the sulfate-binding site, are shown in *blue* characters. The features of Ser-185 (*orange*), Thr-227 (*pink*), and Phe-328 (*green*) are described in the text. *C*, coordination of Arg residues surrounding the sulfate ion. Arg-183 and Arg-231 directly interact with the sulfate ion. Arg-184 interacts with Glu-360′ of the adjacent subunit, and Arg-372′ interacts with Ser-185 and indirectly interacts with Arg-183 mediated by Glu-369′. Distances are given in Å. *D*, the surface charge near the sulfate-binding site is shown on a space-filling model. *Red, blue*, and *gray* colors indicate acidic, basic, and neutral areas, respectively. These structures are drawn from the same angle.

Site-directed Mutagenesis—Site-directed mutagenesis was carried out by the overlap extension method using PCR (30). The pairs of primers used for substitution of amino acids were as follows: 5′-CATCCCACGCAGTCCGCCCagCGCTCG-3′ and 5′-GGAGCGAGCGctGGGCGGACTGCG-3′ for pTMR183Q; 5′-GTCCGCCCGCCagTCGCTCCTGC-3′ and 5′-CTGCAGGAGCGActGGCGGGCGG-3′ for pTMR184Q; 5′-CCCACGCAGTCCGCCCagCagTCGCTCC-3′ and 5′-GCAGGAGCGActGctGGGCGGACTGCG-3′ for pTMR183Q/R184Q; 5′-CTGATGAAATCcaGAGGGCACAACCC-3′ and 5′-GGTGGGTTGTGCCCTCtgGATTTCATC-3′ for pTMR231Q; and 5′-CCAAACGAGCCCTACCaGGTGATACTAGGC-3′ and 5′-CTAGTATCACCtGGTAGGGCTCGTTTGG-3′ for pTMR372Q. The upstream and downstream primers were 5′-CTCGTGTCCGAGGTCGGCAAGTCC-3′ and 5′-CTGTGGAGCTCTTCGGCACGAACA-3′ (for pTMR183Q, pTMR184Q, pTMR183Q/R184Q, and pTMR231Q) and 5′-CCTAAGTTCTTGCGCCGTGTGG-3′ and 5′-CCGTCACACGGATGGACCCGT-3′ (for pTMR372Q). The mutation sites are described in lowercase letters. The plasmid pTM94 was used as a template, and amplification was performed by *KOD-plus* DNA polymerase according to the manufacturer's protocol. After cloning of the amplified mutagenic fragments into pBluescript KS(−)/EcoRV, the sequences of the fragments were confirmed. The cloned fragments then were excised by double digestion with BstPI and NspV and inserted into the BstPI-NspV site of pTM94 (for pTMR183Q, pTMR184Q, pTMR183Q/R184Q, and pTMR231Q). The plasmid pTMR372Q was constructed in the same way as above using Tth111I-ClaI fragments. For high level expression and convenient purification of the recombinant enzymes, the NcoI-HindIII fragments containing the full coding region of PEPC were cut out from pTMR183Q, pTMR184Q, pTMR183Q/R184Q, pTMR231Q, and pTMR372Q. Then the coding region of the wild-type PEPC in a pET plasmid, pEM94, was replaced by these mutant fragments to produce pEMR183Q, pEMR184Q, pEMR183Q/R184Q, pEMR231Q, and pEMR372Q.

Expression and Purification of Recombinant PEPCs—The cells of *E. coli* F15, a *recA* variant of the *ppc* deletion mutant (31), which had

been transformed with pTM94 or the mutant plasmids derived from it, were grown in a minimal glucose-salts medium for complementation testing. If a PEPC coded by the introduced plasmid exerts enough activity in cells, the phenotype of the glutamate requirement is complemented (25). For the preparation of PEPCs for enzymological studies, the transformants (BL21/pEM94, BL21/pEMR183Q, BL21/pEMR184Q, BL21/pEMR183Q/R184Q, BL21/pEMR231Q, and BL21/pEMR372) were first spread on an LB plate containing ampicillin (100 μg ml^{-1}). A single colony of each transformant was selected, inoculated into 20 ml of LB supplemented with 100 μg ml^{-1} ampicillin, and incubated with shaking at 37 °C overnight. The culture was added to 1 liter of LB and incubated with shaking at 37 °C until the OD_{660} reached 0.6. The expression of the fusion protein was induced by the addition of 1 mM isopropyl-1-thio-β-D-galactoside and grown at 25 °C for 4–6 h. The cells collected by centrifugation were washed once with a Wash Buffer (100 mM Tris-HCl (pH 7.6), 20% (v/v) glycerol, 1 mM phenylmethanesulfonyl fluoride, and 14 mM 2-mercaptoethanol), resuspended in 15 ml of Wash Buffer, and then disrupted with a French press (Ohtake Seisakusho Co.). The cell lysate was centrifuged at 20,000 × *g* for 20 min, and the supernatant was fractionated with 30–60% saturated ammonium sulfate. The resulting protein precipitate was dissolved in a Start Buffer (20 mM sodium phosphate buffer (pH 7.4), 0.1 M NaCl, 10 mM imidazole, 20%(v/v) ethylene glycol, 14 mM 2-mercaptoethanol) and filtered through a 0.45-μm filter (Millipore). The solution was loaded on a Ni^{2+}-chelated HiTrap Chelating HP column (1 ml) (Amersham Biosciences). The fusion enzyme was eluted with 10 ml of Elution Buffer (20 mM sodium phosphate buffer (pH 7.4), 0.1 M NaCl, 200 mM imidazole, 20%(v/v) ethylene glycol, 14 mM 2-mercaptoethanol), and the eluate was then collected in two 5-ml fractions. The first 5-ml fraction contained most of the purified protein, as determined by absorption at 280 nm as well as the presence of the expected 127-kDa band (with 17 kDa tags) on an SDS-PAGE (data not shown). This fusion protein was collected and precipitated with 60% saturated ammonium sulfate with an ammonium sulfate-saturated buffer (100 mM Tris-HCl (pH 7.6), ammonium sulfate) at 4 °C overnight. The fusion protein was collected by centrifugation at 20,000 × *g* for 20 min, dissolved in Storage Buffer (25 mM Tris-HCl (pH 7.6), 30% (v/v) ethylene glycol) (32), and kept at −20 °C. Each 1 liter of bacterial culture yielded ~2 mg of ~98% pure protein. The purified enzymes were stable for at least 10 days under these conditions. Before use, the fusion enzyme solution was freed from ethylene glycol by a Sephadex G-50 Fine (Amersham Biosciences) spin column, which had been equilibrated with Wash Buffer and then incubated for 1 h on ice in the presence of 1 mM DTT for full reactivation.

Trimming of Tag Polypeptide from Fusion Protein of PEPC—Because the PEPC was expressed as a fusion protein by the pET system (Novagen) using pET32-a as a vector (24), the N-terminal tag of 159 amino acid residues was trimmed off by rEK for most experiments. The digestion mixture contained, in a total volume of 60 μl, 10 mM Tris-HCl (pH 8.0), 10 mM $CaCl_2$, 0.5% (v/v) glycerol, 1% (v/v) ethylene glycol, 5 mM Gly, 10 mM L-malate (pH 7.4), 1 mM DTT, 80 μg of fusion PEPC, and 0.2 units of rEK. After the mixture was incubated at 30 °C for 4 h, the reaction was terminated by adding 1 mM 4-(2-aminoethyl)benzenesulfonyl fluoride (Pefabloc SCv, Roche Applied Science). The digested products were applied to a Sephadex G-50 Fine spin column for removal of the short tag polypeptide.

In Vitro Regulatory Phosphorylation of PEPC—Phosphorylation reactions were carried out at 25 °C for 1 h in a reaction mixture (80 μl in total) containing 0.1 mM ATP, 2 mM $MgCl_2$, 50 mM Tris-HCl (pH 8.0), 0.04% (w/v) Tween 20, 20 mM DTT, 4 μg of recombinant *Flaveria trinervia* PEPC-k (14), and 40 μg of PEPC. At various intervals 10-μl aliquots of the reaction mixture were withdrawn and added to tubes containing 5 μl of 500 mM EDTA to stop the reaction. The phosphorylation was monitored by Western blot analysis using antibodies specific to the phosphorylated Ser-15 of ZmPEPC (23). The secondary antibody was the peroxidase-conjugated goat anti-rabbit IgG (H + L), and the signals were detected as chemiluminescence by the use of BMG chemiluminescence blotting substrate for peroxidase (Roche Applied Science) with LAS-1000plus (Fuji Film). To quantitate the extent of phosphorylation per mol of subunit, phosphorylation was monitored by the incorporation of radioactive phosphate into PEPC from [γ-^{32}P]ATP. The reaction mixture was the same as described above except for the use of 0.1 mM [γ-^{32}P]ATP (0.5 μCi). Procedures for the measurement of ^{32}P incorporation into PEPC were the same as described previously (14).

Measurement of PEPC Activity—PEPC activity was measured by a coupled spectrophotometric method (33) with some modifications in a Shimadzu UV-2500 PC. One unit of the enzyme activity was defined as 1 μmol of oxaloacetate formed per min at 30 °C. The standard assay mixture contained, in a total volume of 1.0 ml, 100 mM Hepes-NaOH (pH 7.3), 2 mM PEP, 10 mM $KHCO_3$, 10 mM $MgSO_4$, 0.1 mM NADH, 1.5 units of malate dehydrogenase, and the enzyme (0.5–1 μg). The reaction was initiated by the addition of PEP. The protein concentration was routinely determined using a protein assay kit (Bio-Rad) based on dye binding (34) with crystalline bovine serum albumin as a standard. When necessary, the molar concentration of the ZmPEPC subunit was estimated from its molar extinction coefficient at 280 nm, *i.e.* 7.5×10^4 M^{-1} cm^{-1}. The value had been determined previously by amino acid analysis of the acid hydrolysate of PEPC in a solution of known absorbance.[2] (More simply, the PEPC concentration of 1.0 mg per ml estimated by the dye-binding method as above corresponds to an absolute concentration of 0.72 mg per ml, and this solution gives an absorbance of 0.500 at 280 nm.

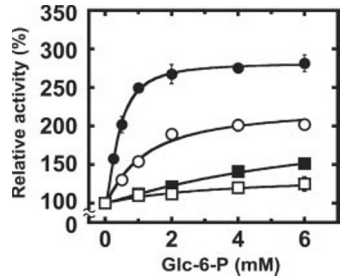

FIG. 3. **Diminished sensitivity of ZmPEPC to Glc-6-P in the presence of high concentrations of ammonium sulfate.** The sulfate-free assay mixture contained, in a total volume of 1.0 ml, 100 mM Tris acetate (pH 7.4), 10 mM $Mg(CH_3COO)_2$, 10 mM $KHCO_3$, 1 mM PEP, 0.1 mM NADH, 1.5 units of malate dehydrogenase, and wild-type PEPC (6 μg). Saturation curves for Glc-6-P were obtained in the absence (●) and presence of 10 mM (○), 100 mM (■) and 200 mM (□) ammonium sulfate. The activities measured in the absence of Glc-6-P and in the presence of increasing concentrations of ammonium sulfate were 11.9, 11.6, 6.9, and 4.7 units mg^{-1} PEPC, in the order as described above.

Analysis of Enzyme Kinetic Data—Calculation of PEPC kinetic constants was performed by fitting the initial velocities to the appropriate equation described below using the commercial computing program Kaleidagraph (Synergy software, version 3.52) (35). Kinetic data were fitted to Equation 1 for substrate and to Equation 2 and Equation 3 for activator and inhibitor respectively,

$$v = V_{max}[S]^n/(S_{0.5}^n + [S]^n) \quad \text{(Eq. 1)}$$

$$v = v_0 + \{(v_{a,max} - v_0)[A]^n/(A_{0.5}^n + [A]^n)\} \quad \text{(Eq. 2)}$$

$$v = v_0 - \{(v_0 - v_{i,min})[I]^n/(I_{0.5}^n + [I]^n)\} \quad \text{(Eq. 3)}$$

where v is the initial velocity; V_{max} is the apparent maximal velocity; $S_{0.5}$ and $A_{0.5}$ are the concentrations of substrate S and activator A, respectively, giving an apparent half of the maximal velocity; n is the Hill coefficient; $v_{a,max}$ is the highest velocity attainable at saturating activator concentrations; $v_{a,min}$ is the lowest velocity attainable at saturating inhibitor concentration; and $I_{0.5}$ is the concentration of an inhibitor I at apparent half-maximum inhibition.

RESULTS

Functional Competition between Glc-6-P and Sulfate—Although the binding of the sulfate anion with PEPC was ascertained by x-ray crystallographic analysis, there have been no functional data suggesting that the sulfate-binding site is identical with the allosteric regulatory site for Glc-6-P. If sulfate behaves simply as an analogue of the phosphate group, the binding sites for Glc-6-P and PEP would both be candidates for binding with sulfate. Thus kinetic experiments were performed to investigate the effect of increasing concentrations of ammonium sulfate on the saturation curves of Glc-6-P and PEP. As shown in Fig. 3, the activation by Glc-6-P tended to diminish with an increase of ammonium sulfate concentration, and almost complete desensitization was brought about at the concentration of 0.2 M, the concentration at which crystallization had been carried out (20). On the other hand, a robust PEP dependence could be observed, and the $S_{0.5}$ and V_{max} values in

[2] Y. Ueno, Y. Yagi, and K. Izui, unpublished data.

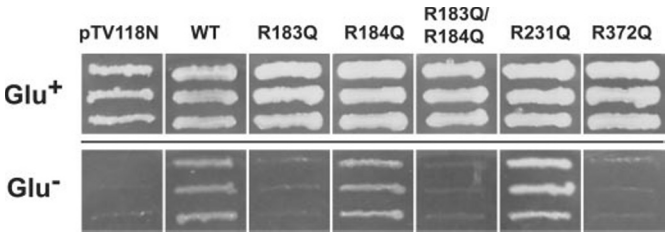

FIG. 4. **Complementation tests of wild-type and mutant PEPCs for growth of *E. coli* F15 (Δ*ppc*).** Wild-type (*WT*) or mutant PEPCs (R183Q, R184Q, R183Q/R184Q, R231Q, and R372Q) were introduced into a deletion mutant of *E. coli* F15, and the growth of each transformant was monitored for 2 days on a minimal agar medium supplemented with Glu (*upper panels*) or without Glu (*lower panels*). As a negative control, a transformant of *E. coli* F15 harboring an empty plasmid, pTV118N, is shown.

the presence of 0.2 M ammonium sulfate were decreased to 67 and 31% of those measured in the absence of sulfate (data not shown). These results strongly suggest that the site for Glc-6-P was occupied by sulfate, but the site for PEP was not under the crystallization conditions. An apparent decrease of the $S_{0.5}$ value was rather unexpected under the conditions of high ionic strength. This could reflect an allosteric-type behavior caused by sulfate bound at the site for Glc-6-P. We had earlier made similar observations regarding *E. coli* PEPC, whose allosteric activator is fructose 1,6-bisphosphate (Fru-1,6-P_2) instead of Glc-6-P (37, 38).

Preparation of Mutant Enzymes—As shown in Fig. 2, the basic residues located at or near the sulfate-binding site are Arg-183, Arg-184, Arg-231, and Arg-372′ (of adjacent subunit). We replaced these Arg residues individually, and in combination for the consecutive residues, with Gln residues. Gln residue was chosen because its physicochemical properties were the most similar to the Arg residue except for its electric charge. The mutant enzymes are denoted as R183Q, R184Q, R231Q, R372Q, and R183Q/R184Q hereafter. First, in order to test the activities of these mutant enzymes *in vivo*, a complementation test was performed with an *E. coli* mutant (F15) in which the gene for PEPC (*ppc*) was deleted as described under "Experimental Procedures." For the expression of wild-type (WT) and mutant PEPCs, a cDNA expression vector of pTV119N (Takara Bio, Inc.) was employed. The plasmid pTM94 carries the cDNA for WT ZmPEPC (33). As shown in Fig. 4, WT, R184Q, and R231Q were able to complement, whereas R183Q, R183Q/R184Q, and R372Q could not (data not shown). Thus, the latter three mutant enzymes were not sufficiently active to support the growth or were not stable enough to be accumulated in the F15 cells.

The WT and mutant enzymes were expressed in the pET system and purified to homogeneity as described under "Experimental Procedures". Because Arg-372′ on the adjacent subunit is located at the interface of two monomers in close contact and can interact with Ser-185 of the counter subunit (20) (Fig. 2, *B* and *C*), a tetrameric structure was suspected to be destabilized in R372Q. In fact, gel filtration analysis of the purified R372Q enzyme (Smart System with a Superose 6 column; Amersham Biosciences) showed a weak tendency of dissociation to give a small peak that presumably corresponded to a monomer, but more than 90% of the enzyme retained a tetrameric structure (data not shown).

Although the enzyme purified with a Ni^{2+}-affinity column is a fusion protein having tags of 159 amino acid residues at the N terminus, our previous studies (26, 27) had shown that the kinetic properties are not significantly affected by the tag peptide. Accordingly, several preliminary experiments were performed with enzymes having tag peptides. However, for most experiments, enzymes whose tag peptide had been trimmed off

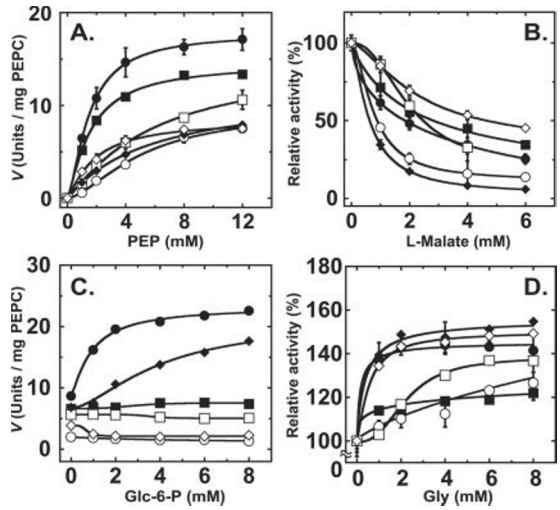

FIG. 5. **Effects of mutations on the saturation curves of PEP (*A*) and allosteric effectors (*B–D*).** The saturation curves for wild-type PEPC (●), R183Q (○), R184Q (■), R183Q/R184Q (□), R231Q (♦), or R372Q (◇) are given. The concentration of PEP was 2 mM for *B–D*. The inhibition curve by L-malate and the activation curve by Gly are expressed as relative activity taking the activity in the absence of effectors as 100% (*B* and *D*). These effects for allosteric effectors are measured independently 2–3 times.

with rEK were used to avoid possible interference by excessive tags. Each tag-trimmed enzyme prepared as described under "Experimental Procedures" was smaller in size, as revealed by SDS-PAGE, and could be sufficiently phosphorylated by PEPC-k, as judged by Western blotting analysis with antibodies specific to the phosphorylated PEPC (23) (data not shown). Kinetic parameters such as V_{max}, $S_{0.5}$, and Hill coefficient (n) for PEP were confirmed not to be affected by the trimming (data not shown).

Saturation Curves for PEP and the Individual Effectors—As shown in Fig. 5*A* and Table I, all the mutant enzymes were catalytically active. The V_{max} attainable at infinite concentration of PEP ranged from 44 to 84% of the V_{max} of WT enzyme. The $S_{0.5}$ (PEP) values were not changed for the mutant enzymes R184Q and R372Q but were increased about 3-fold for R183Q, R183Q/R184Q, and R231Q. The Glc-6-P saturation curves were determined for the wild-type and mutant enzymes in the presence of PEP at a concentration of 2 mM, which is almost equal to or below their $S_{0.5}$ measured in the absence of effector. This concentration of PEP was selected because Glc-6-P exerts a larger influence on the activity of the enzyme. As shown in Fig. 5*C*, all mutant enzymes except for R231Q showed almost complete desensitization to Glc-6-P. For the R231Q enzyme, the curve was slightly sigmoidal, and an apparent $A_{0.5}$ (Glc-6-P) was about 3-fold larger than the WT enzyme. However, the maximum extent of activation was almost the same between both enzymes.

The saturation curves of another activator Gly showed that all the mutant enzymes more or less retained their sensitivity to Gly (Fig. 5*D*). The maximal extent of activation was decreased considerably for the R184Q enzyme, and $A_{0.5}$ (Gly) increased more than 5-fold for the R183Q and R183Q/R184Q enzymes. The curve was strongly sigmoidal for the R183Q/R184Q enzyme.

The influence of an allosteric feedback inhibitor, L-malate, was investigated. Although all the mutant enzymes retained sensitivity to L-malate, sensitivities changed variously for each enzyme (Fig. 5*B* and Table II). For the mutant R183Q and R231Q enzymes, $I_{0.5}$ (L-malate) decreased 2–3-fold compared with the WT enzyme, whereas for the mutant R184Q and R372Q enzymes, the $I_{0.5}$ values increased 1.6- and 2.8-fold,

TABLE I

Effect of allosteric activators (Glc-6-P and Gly) and regulatory phosphorylation on the PEP saturation kinetics for the mutant PEPCs

Kinetic parameters were obtained as described under "Experimental Procedures." Enzyme preparations were assayed with at least five different concentrations of the substrate PEP. The kinetic parameters $S_{0.5}$, V_{max}, and the Hill coefficient (n) were determined using nonlinear regression analysis. Values ± S.D. were estimated by the best fit to Equation 1. The $S_{0.5}$ values are given in mM, and V_{max} values are given as units mg^{-1}. One unit of enzyme catalyzes the oxidation of 1 μmol of NADH min^{-1} in a coupled spectrophotometric assay at 30 °C. The concentrations of Glc-6-P and Gly included in the standard reaction mixture were each 5 mM. The data obtained with the nonphosphorylated PEPCs are denoted as −P and those with phosphorylated PEPC as +P. The phosphorylated PEPCs were prepared as described under "Experimental Procedures."

Enzyme	Phosphorylation state	Allosteric activator present in the assay mixture								
		None			+Glc-6-P			+Gly		
		$S_{0.5}$	V_{max}	n	$S_{0.5}$	V_{max}	n	$S_{0.5}$	V_{max}	n
Wild type	−P	1.8 ± 0.2	19.8 ± 1.6	1.1 ± 0.2	1.1 ± 0.0	31.9 ± 0.9	1.1 ± 0.1	1.1 ± 0.0	25.0 ± 0.3	1.0 ± 0.1
	+P	0.5 ± 0.1	18.0 ± 0.1	1.1 ± 0.0	0.4 ± 0.0	26.4 ± 0.3	1.1 ± 0.0	0.4 ± 0.0	21.1 ± 0.3	1.0 ± 0.1
R183Q	−P	6.5 ± 0.4	10.9 ± 2.4	1.5 ± 0.1	6.8 ± 0.1	10.0 ± 0.9	1.5 ± 0.0	6.1 ± 0.2	12.0 ± 0.3	1.1 ± 0.0
	+P	3.9 ± 0.3	11.7 ± 0.6	1.4 ± 0.1	4.3 ± 0.7	12.0 ± 0.2	1.6 ± 0.2	2.9 ± 0.1	10.1 ± 0.6	1.4 ± 0.1
R184Q	−P	2.2 ± 0.3	16.7 ± 0.7	1.0 ± 0.1	1.9 ± 0.1	17.0 ± 0.3	1.0 ± 0.0	0.9 ± 0.0	14.4 ± 0.0	1.0 ± 0.1
	+P	1.9 ± 0.1	16.7 ± 0.5	1.1 ± 0.1	1.5 ± 0.1	15.0 ± 0.8	1.0 ± 0.0	0.7 ± 0.0	15.3 ± 0.2	0.9 ± 0.1
R183Q/R184Q	−P	6.3 ± 0.5	15.0 ± 1.0	1.2 ± 0.1	5.5 ± 0.4	15.1 ± 0.2	1.3 ± 0.0	3.4 ± 0.4	14.0 ± 0.3	1.4 ± 0.1
	+P	7.6 ± 0.3	15.9 ± 1.0	1.1 ± 0.0	6.4 ± 0.2	15.0 ± 0.6	1.2 ± 0.1	4.0 ± 0.4	13.6 ± 0.1	1.2 ± 0.2
R231Q	−P	6.1 ± 0.3	12.0 ± 0.0	1.0 ± 0.0	1.2 ± 0.0	17.6 ± 0.3	1.3 ± 0.1	0.8 ± 0.1	11.7 ± 0.8	0.8 ± 0.1
	+P	8.6 ± 0.1	17.6 ± 0.2	1.0 ± 0.0	1.5 ± 0.0	18.5 ± 0.1	1.3 ± 0.0	1.2 ± 0.0	11.9 ± 0.3	1.0 ± 0.0
R372Q	−P	1.5 ± 0.2	8.8 ± 0.5	1.0 ± 0.0	1.5 ± 0.0	8.8 ± 0.0	1.0 ± 0.0	0.8 ± 0.1	8.6 ± 0.4	1.0 ± 0.1
	+P	3.0 ± 0.2	9.7 ± 0.2	1.0 ± 0.0	1.3 ± 0.0	7.7 ± 0.4	1.0 ± 0.2	1.0 ± 0.0	7.3 ± 0.6	1.0 ± 0.1

TABLE II

Effect of allosteric activators (Glc-6-P and Gly) and regulatory phosphorylation on the L-malate saturation kinetics for the mutant PEPCs

Kinetic parameters were obtained as described under "Experimental Procedures." Enzyme preparations were assayed with at least five different concentrations of the inhibitor L-malate. The kinetic parameters $I_{0.5}$, $v_{i,min}$, and the Hill coefficient (n) were determined using nonlinear regression analysis. Values ± S.D. were estimated by the best fit to Equation 3. The $I_{0.5}$ values are given in mM, and the maximum extent of inhibition (I_{max}) was given as % calculated according to $(1 - v_{i,min}/v_0) \times 100$. Enzyme assay was performed as described in Table I. The concentrations of Glc-6-P and Gly included in the standard reaction mixture were 5 mM each. The data obtained with the nonphosphorylated PEPCs are denoted as −P and those with phosphorylated PEPC as +P. The phosphorylated PEPCs were prepared as described under "Experimental Procedures."

Enzyme	Phosphorylation state	Allosteric activator present in the assay mixture								
		None			+Glc-6-P			+Gly		
		$I_{0.5}$	I_{max}	n	$I_{0.5}$	I_{max}	n	$I_{0.5}$	I_{max}	n
Wild type	−P	1.8 ± 0.2	100	0.9 ± 0.2	6.6 ± 1.9	59	1.4 ± 0.2	22.1 ± 0.0	70	1.6 ± 0.0
	+P	8.1 ± 0.7	100	1.4 ± 0.0	10.2 ± 0.1	72	1.2 ± 0.3	13.1 ± 0.1	58	1.4 ± 0.1
R183Q	−P	0.8 ± 0.0	87	1.8 ± 0.3	0.6 ± 0.1	89	1.5 ± 0.1	0.3 ± 0.0	76	1.1 ± 0.1
	+P	0.7 ± 0.1	81	1.4 ± 0.4	0.7 ± 0.1	87	1.4 ± 0.4	1.1 ± 0.2	86	1.4 ± 0.3
R184Q	−P	2.9 ± 0.3	100	1.0 ± 0.1	1.4 ± 0.1	100	0.7 ± 0.0	9.5 ± 0.1	100	1.7 ± 0.1
	+P	5.7 ± 0.4	100	0.9 ± 0.0	3.4 ± 0.1	68	1.2 ± 0.1	40.2 ± 1.0	100	2.1 ± 0.1
R183Q/R184Q	−P	2.9 ± 0.1	100	1.5 ± 0.2	2.0 ± 0.0	100	0.9 ± 0.2	7.0 ± 0.1	58	1.0 ± 0.2
	+P	3.3 ± 0.0	100	1.7 ± 0.3	0.6 ± 0.1	76	1.1 ± 0.1	1.7 ± 0.2	63	1.5 ± 0.4
R231Q	−P	0.6 ± 0.0	100	1.2 ± 0.0	0.9 ± 0.0	100	1.6 ± 0.0	2.8 ± 0.1	100	1.5 ± 0.1
	+P	0.8 ± 0.0	100	1.2 ± 0.0	0.8 ± 0.1	100	1.5 ± 0.1	2.3 ± 0.0	100	1.6 ± 0.1
R372Q	−P	5.0 ± 0.8	100	1.0 ± 0.1	4.7 ± 0.3	100	1.0 ± 0.1	31.8 ± 1.2	100	2.8 ± 0.4
	+P	8.0 ± 1.1	100	0.7 ± 0.1	5.1 ± 0.2	100	0.7 ± 0.2	30.4 ± 0.6	100	1.1 ± 0.1

respectively. Again an apparently sigmoidal saturation curve was obtained for the R183Q/R184Q enzyme with an increased $I_{0.5}$ value. The accentuated cooperativity for both activator and inhibitor seemed rather strange from the simple two-state concerted allosteric transition model applied to maize PEPC (36). If we assume the appearance of another but predominant conformational state (T′-state) between the usual T- and R-states, in which constraint on subunit interaction is the strongest among the three states, kinetic description may be possible for this double mutant enzyme. Further molecular analysis of these kinetic properties remains to be elucidated. The "three-state allosteric model" for *E. coli* PEPC has been discussed previously to explain atypical allosteric kinetics (39). An asymptotic value of v on the hemi-reciprocal plot (v^{-1} *versus* [I]) of the data indicated that the maximum extent of inhibition is 90% for the R183Q enzyme, whereas for the other enzymes it is almost 100%.

Influence of Allosteric Effectors on Saturation Curves of PEP and L-Malate—The empirical kinetic parameters of PEP and L-malate for the WT and mutant enzymes are summarized in Tables I and II, respectively, and several representative saturation curves are depicted for the WT and R372Q enzymes in Fig. 6. For the WT enzyme, V_{max} and $S_{0.5}$ increased about 1.5-fold and decreased to 60%, respectively, by the addition of 5 mM Glc-6-P. Similar effects were observed also with Gly (Fig. 6*A*). On the other hand, for the R372Q enzyme, no effect was seen with Glc-6-P, but a decrease in $S_{0.5}$ was also observed with Gly (Fig. 6*C*). The inhibition curves obtained similarly in the presence of individual activators (Fig. 6, *B* and *D*) showed again that the effect of Glc-6-P was abolished but that of Gly was retained for the mutant enzyme. R231Q does indeed behave like WT to Glc-6-P in PEP saturation kinetics (Table I) but not for malate inhibition (Table II).

Influence of Regulatory Phosphorylation—To investigate whether the ability of PEPC to respond to regulatory phosphorylation was affected or not by the mutations that had brought about desensitization to Glc-6-P, all the mutant enzymes as well as the WT enzyme were phosphorylated by PEPC-k of *F. trinervia* (14). As already reported, the WT enzyme (ZmPEPC) could be phosphorylated, but a mutant enzyme whose Ser at the phosphorylation site had been replaced by Ala (S15A) could not, confirming the specificity of the kinase (data not shown). The effect of each ligand on phosphorylation was next examined with the WT enzyme to ascertain the conditions for full phosphorylation of PEPC. As shown in Fig. 7, ^{32}P incorporation proceeded with time, and the highest extent of

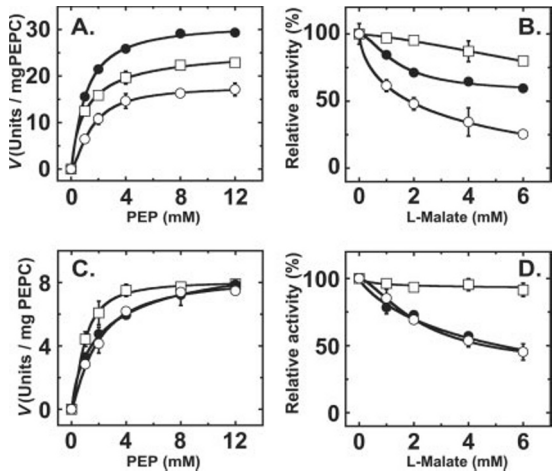

FIG. 6. **Saturation curves of PEP (*A* and *C*) and L-malate (*B* and *D*) in the presence of allosteric activators.** Activities of wild-type (*A* and *B*) and a mutant enzyme, R372Q (*C* and *D*), were measured in the absence of activators (○), in the presence of 5 mM Glc-6-P (●), or in presence of 5 mM Gly (□). Measurements were made independently 2–3 times.

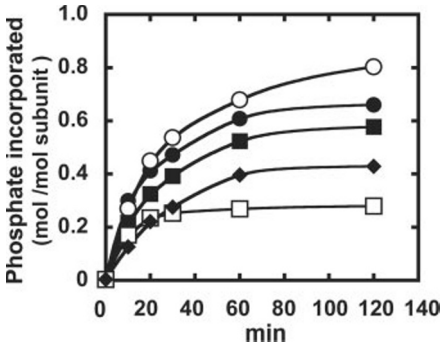

FIG. 7. **Effect of ligands on the regulatory phosphorylation of PEPC by PEPC-k.** Time course of PEPC phosphorylation using [γ-^{32}P]ATP in the absence of ligand (●), in the presence of 1 mM DCDP (○), 10 mM Glc-6-P (■), 10 mM Gly (□), or 15 mM L-malate (♦) was followed, using WT PEPC with a short tag peptide produced by an expression plasmid pET30a-PEPC (K. Ohshima, T. Furumoto, and K. Izui, unpublished observations). Incorporation of ^{32}P into PEPC with a recombinant *F. trinervia* PEPC-k was measured as described under "Experimental Procedures."

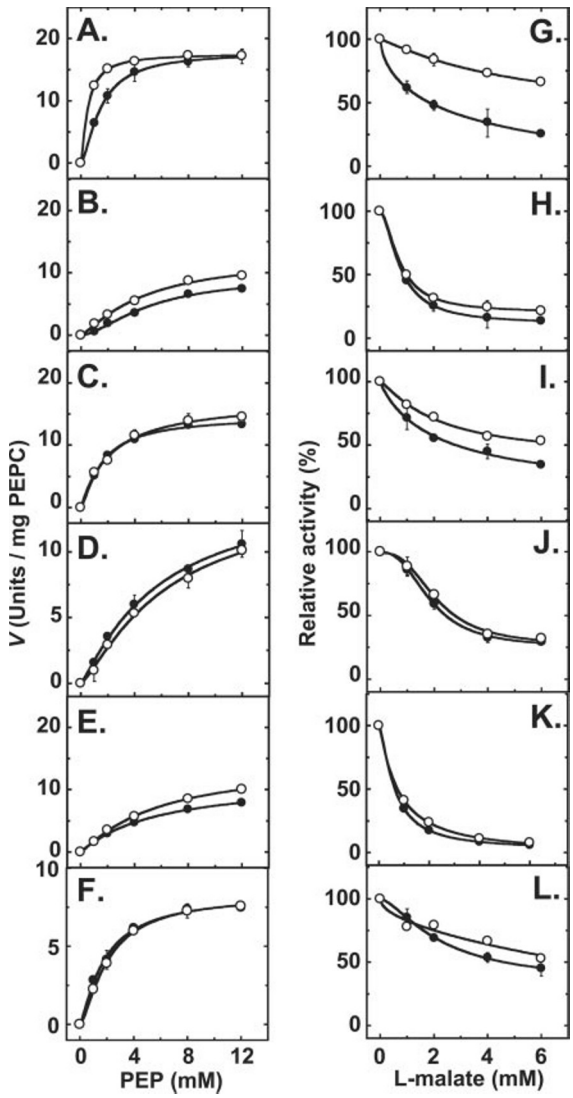

FIG. 8. **Effect of phosphorylation on the saturation curves of PEP (*A–F*) and L-malate (*G–L*).** The recombinant enzymes without a tag peptide were prepared and phosphorylated as described under "Experimental Procedures." Activities of nonphosphorylated (●) and phosphorylated (○) PEPCs were measured: wild-type (*A* and *G*) and mutant enzymes, R183Q (*B* and *H*), R184Q (*C* and *I*), R183Q/R184Q (*D* and *J*), R231Q (*E* and *K*), and R372Q (*F* and *L*). The measurements were independently performed 2–3 times, and data are given with *error bars*.

phosphorylation was obtained when DCDP, a PEP analogue, was included in the reaction mixture. In contrast, in the presence L-malate, the rate and extent were both significantly low, but in the presence of Gly the initial rate was high but the extent was the lowest. Because the extent of phosphorylation fluctuated from 0.7 to 1.0 per subunit because of experimental difficulties, representative data are shown in Fig. 7. The results indicated that the phosphorylation of PEPC is affected in a complex manner by the ligand types, the mechanism of which remains to be elucidated. Thus the fully phosphorylated form of WT and mutant PEPCs (0.7–1.1 per subunit) could be prepared by the reaction with PEPC-k in the absence of any ligand for 2–3 h at 30 °C. Tables I and II summarize the kinetic properties of the phosphorylated WT and mutant enzymes, and Fig. 8 depicts representative data. Fig. 8*A* shows that the $S_{0.5}$ (PEP) was decreased by phosphorylation for the WT enzyme, whereas such response upon phosphorylation was mostly or completely abolished for the mutant enzymes (Fig. 8, *B–F*). As shown in Fig. 8*G*, the phosphorylation caused a decrease in the sensitivity to L-malate for the WT enzyme, whereas no such response could be seen for these mutant enzymes except for R184Q and R372Q (Fig. 8, *I* and *L*). Tables I and II show that the changes in kinetic parameters brought about by regulatory phosphorylation were negligible or very small in all mutant enzymes as compared with the WT enzyme. These results indicate that the mutant enzymes desensitized to Glc-6-P lost also the ability to be "activated" by regulatory phosphorylation.

DISCUSSION

Arg Residues Involved in the Activation by Glc-6-P—Replacement of Arg residues at 183, 184, 231, and 372 by Gln generated mutant enzymes, which are predominantly desensitized to Glc-6-P, but substantially retained sensitivities to the other effectors. Taken together with the results of functional competition between sulfate and Glc-6-P (Fig. 3), it is highly probable that the sulfate-binding site revealed by x-ray crystallography is the site for the binding with the phosphate group of Glc-6-P. Closer examination of the structure around the sulfate-binding site reveals that not all of the Arg residues directly interact with the sulfate ion (Fig. 2*C*). Arg-183 and Arg-231 are located close enough to directly interact with the sulfate anion, whereas Arg-184 and Arg-

372′ (of the adjacent subunit) are not. It can be presumed that Arg-184 and Arg-372′ contribute indirectly to the sulfate binding through neutralizing the negative charges of Glu-360′ and Glu-369′ of the adjacent subunit, respectively, which are located near the sulfate-binding site. Furthermore, Arg-372′ possibly contributes to keep Ser-185 at the right position together with Arg-183. The OH group of Ser-185 can make a hydrogen bond with the oxygen atom of sulfate. The role of Ser-185 in Glc-6-P sensitivity remains to be elucidated. Although it is usually expected that the single replacement of amino acid residues involved in binding with a ligand should cause a partial decrease (or increase) in the affinity to the ligand, almost complete desensitization to Glc-6-P was observed with R183Q, R184Q, R183Q/R184Q, and R372′Q but not with R231Q. Thus the replacements of the former four mutant enzymes seem to have caused either severe impairment in the ligation with a whole Glc-6-P molecule or damage on the structure necessary for the transmission of the allosteric signal arising from the binding of Glc-6-P. A similar observation has been reported previously (40) with a yeast pyruvate kinase of which the allosteric activator is Fru-1,6-P_2. In this case, the replacement of Arg-459 participating in the binding with the phosphate group of Fru-1,6-P_2 to Gln caused complete desensitization to this effector, indicating that this Arg residue is also involved in allosteric signal transmission (41).

At present, the site for the accommodation of the glucose moiety of Glc-6-P is not clear. Because the binding site of the sulfate ion is located at the edge of the subunit, it may be possible that the site for the glucose moiety is located in the cavity built up of two adjacent subunits, as there seems adequate space to accommodate the glucose moiety. By analogy with the case of the Glc-6-P-binding site in yeast glycogen phosphorylase (42, 43), Phe-328′ of the adjacent subunit may be located at the bottom of the neutral cavity, and a plant-specific loop (348′–369′) from the adjacent subunit may also be involved in the interaction with the glucose moiety of Glc-6-P (Fig. 2, *A–D*). Indeed Arg-372′ and the plant-specific loop mentioned above are contained in the "region II" that had been depicted as a region involved in the evolution of responsiveness to this allosteric activator in accompaniment with the evolution of *Flaveria* genus from C_3 to C_4 plants (44). Thus detailed analysis of this region will provide a clue to the molecular traits of the evolution of the allosteric activation in plant PEPC. A molecular modeling study showing a good accommodation of Glc-6-P at the sulfate-binding site on ZmPEPC is being carried out, and will be published elsewhere by Mancera and Carrington.[3]

A Thr Residue Near Arg-18—In most bacterial PEPCs, Fru-1,6-P_2 is an allosteric activator instead of Glc-6-P (10). Because all Arg residues examined in this study are conserved in *E. coli* PEPC as shown in Fig. 1, one of the phosphate groups of Fru-1,6-P_2 is thought to interact with some of these Arg residues. The binding site for another phosphate group remains to be elucidated. It has been reported that a mutant PEPC of *E. coli* whose Thr-188 was altered to Ile almost completely lost sensitivity to Fru-1,6-P_2 (45). Because Thr-188, which corresponds to Thr-227 in ZmPEPC, is located close to Arg-183, as shown in Fig. 2*B*, the residue may participate in the formation of the binding site for sugar phosphate or in the transmission of the allosteric regulatory signal.

Gly Binding Site Is Distinct from Glc-6-P-binding Site—Gly is known to be an allosteric activator for PEPC from monocot plants. In the WT enzyme the inhibition by L-malate was greatly relieved by Gly (Table II). Because R184Q, R231Q, and R372Q retained sensitivity to Gly, the binding site for Gly seems distinct from the site for Glc-6-P, as pointed out previously (46–48). However, it should be noted that, among all mutants, Gly sensitivity was most severely diminished in R183Q (Tables I and II), indicating the multiple role of Arg-183 in the transmission of allosteric regulatory signals in the molecule. The site for Gly binding remains to be elucidated.

TABLE III
Kinetic parameters of Glc-6-P for PEPC, which had been phosphorylated to various extents

The $A_{0.5}$ values, maximum extents of activation, and the Hill coefficients were measured with the WT PEPC. The phosphorylation was carried out with PEPC-k in the absence of any ligand of PEPC, as described under "Experimental Procedures." The extent of phosphorylation was measured by the use of [γ-^{32}P]ATP as described under "Experimental Procedures." Saturation curves of Glc-6-P were obtained with the same standard assay mixture except for PEP concentration (0.2 mM).

Phosphate incorporated into PEPC	$A_{0.5}$	Maximum activation[a]	Hill coefficient
mol P/mol subunit	*mM*	*%*	*n*
0.0	1.9 ± 0.2	490	2.2 ± 0.4
0.3	2.5 ± 0.0	490	1.9 ± 0.2
0.5	2.1 ± 0.1	450	1.8 ± 0.2
0.7	2.5 ± 0.2	450	1.4 ± 0.0
0.8	2.0 ± 0.1	380	1.8 ± 0.2
1.0	1.6 ± 0.2	410	2.1 ± 0.2

[a] The maximum extent of activation by Glc-6-P (activity in the absence of Glc-6-P was taken as 100%).

Desensitization to Regulatory Phosphorylation—An unexpected and novel finding in this study is that the responsiveness of enzyme activity to the regulatory phosphorylation was abolished or severely diminished in the mutant enzymes prepared in this study. The $I_{0.5}$ value for L-malate increased about 4-fold upon phosphorylation for the WT enzyme, whereas these values did not increase at all or increased 2-fold at most for the mutant enzymes (Table II). Similarly the $S_{0.5}$ values for PEP for the mutant enzymes were not as markedly decreased upon phosphorylation as for the WT enzyme (Table I). Previously, a molecular mechanism for the decrease of allosteric inhibition caused by phosphorylation had been proposed by us on the basis of the three-dimensional structure of *E. coli* PEPC (19). It was postulated that, when the flexible N-terminal peptide is phosphorylated at Ser-15, the resulting negatively charged region will occupy the inhibitor-binding site where basic residues are clustered. Although this model can explain why the $I_{0.5}$ value increases upon phosphorylation without assuming global conformational changes, the model cannot explain why the disruption of the Glc-6-P-binding site desensitizes PEPC to phosphorylation. However, if we assume that the phosphate group on Ser-15 causes an enzyme activation through binding at the site for Glc-6-P, this apparent controversy could be reconciled. Inspection of the three-dimensional structure revealed that the phosphate group on Ser-15 seemed to be barely able to reach the sulfate-binding site, if the N-terminal peptide takes an extended structure. In fact, this case is very similar to that of glycogen phosphorylase from yeast. In this enzyme, the nonphosphorylated N-terminal peptide is extended to reach the catalytic site of the adjacent subunit to inhibit the enzyme, and when phosphorylated the N-terminal peptide folds back and the phosphate group is trapped at the allosteric inhibition site for Glc-6-P resulting deinhibition (41). Competition of the binding site between the phosphate group on Ser-15 and Glc-6-P was indeed demonstrated (49). To investigate this possibility for PEPC, $A_{0.5}$ values for Glc-6-P were measured with the WT enzyme that had been phosphorylated to various extents. As

[3] R. L. Mancera and B. J. Carrington, De Novo Pharmaceuticals, personal communication.

shown in Table III, the $A_{0.5}$ value of nonphosphorylated PEPC was not smaller than but rather was equal to the $A_{0.5}$ value of fully phosphorylated PEPC, and the values were transiently bumped along with the increase in the extent of phosphorylation. In case of aspartate transcarbamoylase of *E. coli*, maleate is known to activate the enzyme at a low Asp concentration as an Asp analogue through binding at the vacant catalytic site of the adjacent subunit (50). Previous observation has also showed that the $A_{0.5}$ value of Glc-6-P decreases about 2-fold upon regulatory phosphorylation (35). Thus there seemed no apparent competition between the phosphate group on the N-terminal peptide and Glc-6-P for the common binding site. We must speculate that these four Arg residues are not only involved in the interaction with Glc-6-P but also play a pivotal role in relaying regulatory signals originating upon phosphorylation. Further enzymological work is now in progress to elucidate the molecular mechanism of regulatory phosphorylation.

Acknowledgments—We thank Dr. Shingo Hata for useful suggestions and Dr. Yuhei Tsuchida for providing a recombinant PEPC-k. We also express our gratitude to Ricardo L. Mancera and Benjamin J. Carrington, De Novo Pharmaceuticals, Compass House, Vision Park, Histon, Cambridge CB4 9ZR, UK, for generous permission to mention their work as a personal communication.

REFERENCES

1. Utter, M. F., and Kolenbrander, H. M. (1972) *Enzymes* **6,** 117–168
2. O'Leary, M. H. (1982) *Annu. Rev. Plant Physiol.* **33,** 297–315
3. Chollet, R., Vidal, J., and O'Leary, M. H. (1996) *Annu. Rev. Plant. Physiol. Plant Mol. Biol.* **47,** 273–298
4. Izui, K., Matsumura, H., Furumoto, T., and Kai, Y. (2004) *Annu. Rev. Plant Biol.* **55,** 69–84
5. Latzko, E., and Kelly, G. J. (1983) *Physiol. Veg.* **21,** 805–815
6. Buchanan, B. B., Gruissem, W., and Jones, R. L. (2000) *Biochemistry & Molecular Biology of Plants,* pp. 619–626, American Society of Plant Physiologists, Rockville, MD
7. Buchanan, B. B., Gruissem, W., and Jones, R. L. (2000) *Biochemistry & Molecular Biology of Plants,* pp. 812–815, American Society of Plant Physiologists, Rockville, MD
8. Sako, Y., Takai, K., Nishizaka, T., and Ishida, Y. (1997) *FEMS Microbiol. Lett.* **153,** 159–165
9. Patel, H. M., Kraszewski, J. L., and Mukhopadhyay, B. (2004) *J. Bacteriol.* **186,** 5129–5137
10. Izui, K. (2002) *Enzymes, Lyase* (Izui, K., ed) **4,** 37–49, Hirokawa Publishing Co., Tokyo, Japan
11. Dong, L. Y., Masuda, T., Kawamura, T., Hata, S., and Izui, K. (1998) *Plant Cell Physiol.* **39,** 865–873
12. Svensson, P., Bläsing, O. E., and Westhoff, P. (2003) *Arch. Biochem. Biophys.* **414,** 180–188
13. Vidal, J., and Chollet, R. (1997) *Trends Plant Sci.* **2,** 1360–1385
14. Tsuchida, Y., Furumoto, T., Izumida, A., Hata, S., and Izui, K. (2001) *FEBS Lett.* **507,** 318–322
15. Nimmo, H. G. (2003) *Arch. Biochem. Biophys.* **414,** 189–196
16. Miyao, M., and Fukayama, H. (2003) *Arch. Biochem. Biophys.* **414,** 197–203
17. Chen, L. M., Li, K. Z., Miwa, T., and Izui, K. (2004) *Planta* **219,** 440–449
18. Kai, Y., Matsumura, H., and Izui, K. (2003) *Arch. Biochem. Biophys.* **414,** 170–179
19. Kai, Y., Matsumura, H., Inoue, T., Terada, K., Nagara, Y., Yoshinaga, T., Kihara, A., Tsumura, K., and Izui, K. (1999) *Proc. Natl. Acad. Sci. U. S. A.* **96,** 823–828
20. Matsumura, H., Xie, Y., Shirakata, S., Inoue, T., Yoshinaga, T., Ueno, Y., Izui, K., and Kai, Y. (2002) *Structure* (*Lond.*) **10,** 1721–1730
21. Johnson, L. N., and Barford, D. (1990) *J. Biol. Chem.* **265,** 2409–2412
22. Trapani, S., Linss, J., Goldenberg, S., Fischer, H., Craievich, A. F., and Oliva, G. (2001) *J. Mol. Biol.* **313,** 1059–1072
23. Ueno, Y., Imanari, E., Emura, J., Yoshizawa-Kumagaye, K., Nakajima, K., Inami, K., Shiba, T., Sakakibara, H., Sugiyama, T., and Izui, K. (2000) *Plant J.* **21,** 17–26
24. Jenkins, C. L. D., Harris, R. L. N., and McFadden, H. G. (1987) *Biochem. Int.* **14,** 219–226
25. Yano, M., and Izui, K. (1997) *Eur. J. Biochem.* **247,** 74–81
26. Dong, L. Y., Ueno, Y., Hata, S., and Izui, K. (1997) *Plant Cell Physiol.* **38,** 1340–1345
27. Dong, L. Y., Hata, S., and Izui, K. (1997) *Biosci. Biotechnol. Biochem.* **61,** 545–546
28. Izui, K., Ishijima, S., Yamaguchi, Y., Katagiri, F., Murata, T., Shigesada, K., Sugiyama, T., and Katsuki, H. (1986) *Nucleic Acids Res.* **14,** 1615–1628
29. Yanagisawa, S., Izui, K., Yamaguchi, Y., Shigesada, K., and Katsuki, H. (1988) *FEBS Lett.* **229,** 107–110
30. Ho, S. N., Hunt, H. D., Horton, R. M., Pullen, J. K., and Pease, L. R. (1989) *Gene* (*Amst.*) **77,** 51–59
31. Cunin, R., Boyen, A., Pouels, P., Glansdorff, N., and Crabeel, M. (1975) *Mol. Gen. Genet.* **140,** 51–60
32. Ogawa, N., Kai, T., Yabuta, N., and Izui, K. (1997) *Plant Cell Physiol.* **38,** 76–80
33. Ueno, Y., Hata, S., and Izui, K. (1997) *FEBS Lett.* **417,** 57–60
34. Bradford, M. M. (1976) *Anal. Biochem.* **72,** 248–254
35. Tovar-Méndez, A., Mújica-Jiménez, C., and Muñoz-Clares, R. A. (2000) *Plant Physiol.* **123,** 149–160
36. Frank, J., Clarke, R. J., Vater, J., and Holzwarth, J. F. (2001) *Biophys. Chem.* **92,** 53–64
37. Kodaki, T., Fujita, N., Kameshita, I., Izui, K., and Katsuki, H. (1984) *J. Biochem.* (*Tokyo*) **95,** 637–642
38. Izui, K., Fujita, N., and Katsuki, H. (1982) *J. Biochem.* (*Tokyo*) **92,** 423–432
39. Izui, K. (1970) *J. Biochem.* (*Tokyo*) **68,** 227–238
40. Jurica, M. S., Mesecar, A., Heath, P. J., Shi, W., Nowak, T., and Stoddard, B. L. (1998) *Structure* (*Lond.*) **6,** 195–210
41. Fenton, A. W., and Blair, J. B. (2002) *Arch. Biochem. Biophys.* **397,** 28–39
42. Lin, K., Rath, V. L., Dai, S. C., Fletterick, R. J., and Hwang, P. K. (1996) *Science* **273,** 1539–1542
43. Rath, V. L., Lin, K., Hwang, P. K., and Fletterick, R. J. (1996) *Structure* (*Lond.*) **4,** 463–473
44. Bläsing, O. E., Westhoff, P., and Svensson, P. (2000) *J. Biol. Chem.* **275,** 27917–27923
45. Sutton, F., Butler, E. T., III, and Smith, T. E. (1986) *J. Biol. Chem.* **261,** 16078–16081
46. Bandarian, V., Poehner, W. J., and Grover, S. D. (1992) *Plant Physiol.* **100,** 1411–1416
47. Mújica-Jiménez, C., Castellanos-Martínez, A., and Muñoz-Clares, R. A. (1998) *Biochim. Biophys. Acta.* **1386,** 132–144
48. Podestá, F. E., González, D. H., and Andreo, C. S. (1987) *Plant Cell Physiol.* **28,** 375–378
49. Buchbinder, J. L., Rath, V. L., and Fletterick, R. J. (2001) *Annu. Rev. Biophys. Biomol. Struct.* **30,** 191–209
50. Gerhart, J. C., and Pardee, A. B. (1963) *Cold Spring Harbor Symp. Quant. Biol.* **28,** 491–496